

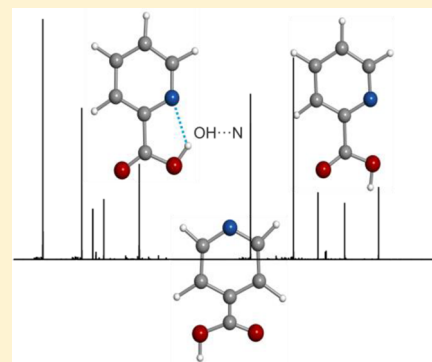
1 Picolinic and Isonicotinic Acids: A Fourier Transform Microwave 2 Spectroscopy Study

3 Isabel Peña, Marcelino Varela, Vanina G. Franco, Juan C. López, Carlos Cabezas, and José L. Alonso*

4 Grupo de Espectroscopia Molecular (GEM), Edificio Quifima, Laboratorios de Espectroscopia y Bioespectroscopia, Unidad Asociada
5 CSIC, Universidad de Valladolid, 47011 Valladolid, Spain

6  Supporting Information

7 **ABSTRACT:** The rotational spectra of laser ablated picolinic and isonicotinic acids
8 have been studied using broadband chirped pulse (CP-FTMW) and narrowband
9 molecular beam (MB-FTMW) Fourier transform microwave spectroscopies. Two
10 conformers of picolinic acid, *s-cis*-I and *s-cis*-II, and one conformer of isonicotinic
11 acid have been identified through the analysis of their rotational spectra. The values
12 of the inertial defect and the quadrupole coupling constants obtained for the most
13 stable *s-cis*-I conformer of picolinic acid, evidence the formation of an O–H···N
14 hydrogen bond between the acid group and the endocyclic N atom. The
15 stabilization provided by this hydrogen bond compensates the destabilization energy
16 due to the adoption of a –COOH trans configuration in this conformer. Its r_s
17 structure has been derived from the rotational spectra of several ^{13}C , ^{15}N , and ^{18}O
18 species observed in their natural abundances. Mesomeric effects have been revealed
19 by comparing the experimental values of the ^{14}N nuclear quadrupole coupling
20 constants in the isomeric series of picolinic, isonicotinic, and nicotinic acids.



21 ■ INTRODUCTION

22 The two isomeric molecules picolinic (pyridine-2-carboxylic
23 acid) and isonicotinic (pyridine-4-carboxylic acid)
24 ($\text{C}_6\text{H}_5\text{NO}_2$) are pyridine derivatives, which have a great interest
25 due to their chemical and biological properties. The isonicotinic
26 acid is a main metabolite of isonicotinic acid hydrazide, which is
27 used as a therapeutic drug for tuberculosis.¹ The picolinic acid
28 is an endogenous metabolite of L-tryptophan, which has been
29 detected in several biological mediums as blood serum,
30 cerebrospinal fluid, human milk, pancreatic juice, and intestinal
31 homogenates.^{2–5} Picolinic acid is also known as a metal
32 chelating agent in the human body. They have been
33 investigated in condensed phases using IR, Raman, and X-ray
34 techniques,^{6–13} but none of them provide a detailed conforma-
35 tional picture about these isomeric species. Hence, the
36 experimental and theoretical vibrational spectra have been
37 interpreted in terms of the wavenumbers and intensities of
38 selected experimental bands,¹¹ which have been compared and
39 discussed on the basis of the position of the nitrogen atom in
40 the aromatic ring. All results indicate that the structural
41 propensities observed in condensed phases are strongly biased
42 by interactions with the solvent or the crystal packing
43 forces.^{12,13}

44 The unambiguous characterization of the intrinsic conforma-
45 tional preferences can be achieved through the analysis of the
46 rotational spectra. Molecules placed in an isolated environment
47 such as that provided by the gas phase, free of the interactions
48 with the solvent, exhibit their intrinsic molecular properties. In
49 the present work we have investigated the rotational spectra of
50 the biological active molecules, picolinic and isonicotinic acids, to

obtain precise information on their conformation and structure. 51
The combination of narrowband molecular beam Fourier 52
transform microwave (MB-FTMW) spectroscopy and broad- 53
band chirped pulse Fourier transform (CP-FTMW) with laser 54
ablation (LA) vaporization provides a powerful experimental 55
tool,^{14,15} which allows the investigation of the rotational spectra 56
of solid biomolecules such as natural amino acids,¹⁶ 57
dipeptides,¹⁷ nucleic acid bases,¹⁸ and monosaccharides¹⁹ in 58
the gas phase. We present here the first experimental rotational 59
studies of picolinic and isonicotinic acids using a combination 60
of the aforementioned techniques. The results have been 61
compared with those previously reported for nicotinic acid 62
(pyridine-3-carboxylic acid), in which two conformers, *s-cis* and 63
s-trans, have been recently unveiled.¹⁴ 64

■ EXPERIMENTAL SECTION

65 Details of the Chirped-pulse Fourier transform microwave (CP- 66
FTMW) spectrometer coupled with a laser ablation source are 67
given elsewhere.¹⁴ Cylindrical rods of picolinic acid (m.p.: 138 68
°C) and isonicotinic acid (m.p.: 310 °C) samples were obtained 69
by pressing a mixture formed by fine powder of the substances 70
with a few drops of a commercial binder, in a hydraulic bench 71
press. They were vaporized in the ablation nozzle of the 72
spectrometer¹⁴ using the third harmonic (355 nm) of a ps 73
Nd:YAG laser (Ekspla, 20 ps 15 mJ/pulse). The vaporized 74
molecules seeded in the carrier gas Ne (stagnation pressure of 75

Received: September 29, 2014

Revised: November 4, 2014

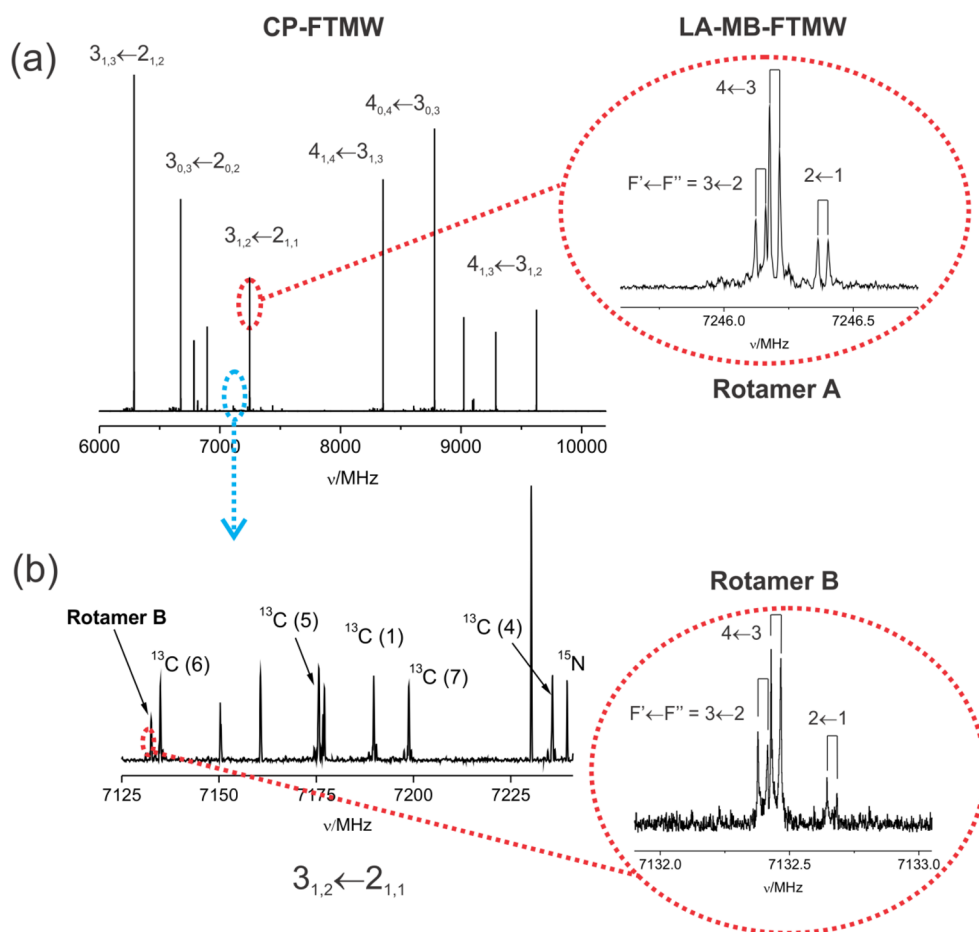


Figure 1. (a) CP-FTMW spectrum of laser ablated picolinic acid showing the groups of μ_a R-branch transitions for rotamer A. The inset shows the quadrupole hyperfine structure for the $3_{1,2} \leftarrow 2_{1,1}$ transition measured with the LA-MB-FTMW spectrometer. (b) The $3_{1,2} \leftarrow 2_{1,1}$ rotational transition for the different isotopic species of rotamer A observed in their natural abundances. The same rotational transition is observed for rotamer B. The resolved quadrupole hyperfine structure by LA-MB-FTMW spectroscopy is also shown in the inset.

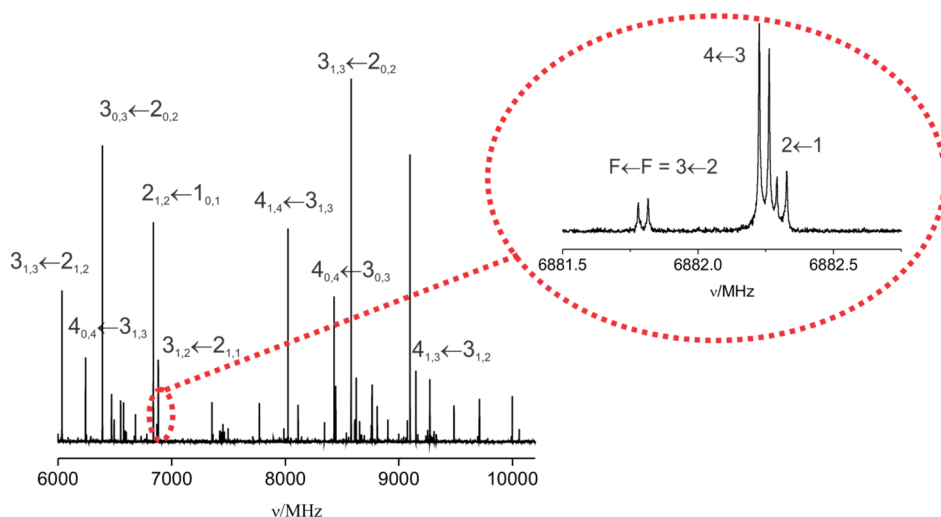


Figure 2. CP-FTMW spectrum of laser ablated isonicotinic acid and the quadrupole hyperfine structure for the $3_{1,2} \leftarrow 2_{1,1}$ rotational transition obtained by LA-MB-FTMW spectroscopy.

76 10 bar) were expanded supersonically into the vacuum chamber
 77 and probed by a microwave chirped pulse. Up to 60 000
 78 individual free induction decays (4 FIDs on each valve cycle)
 79 for picolinic and isonicotinic acids were averaged in the time
 80 domain and Fourier transformed to obtain the frequency

domain rotational spectra from 6 to 10.2 GHz shown in Figures 81 f1
 1 and 2. A Kaiser–Bessel window was applied to increase the 82 f1f2
 baseline resolution. 83

Additional measurements were done using the higher 84
 resolution of our LA-MB-FTMW spectrometer¹⁵ to resolve 85

86 the ^{14}N nuclear quadrupole coupling hyperfine structure. This
87 spectrometer, which works in the 4–12 GHz frequency region,
88 uses a laser ablation system with a ps-laser (Quantel, 35 ps 12
89 mJ/pulse). The vaporized molecules were seeded in Ne at 15
90 bar of pressure and introduced into a Fabry–Pérot resonator to
91 form a supersonic jet. A short microwave radiation pulse (0.3
92 μs) was then applied to macroscopically polarize the molecules
93 in the beam. The subsequent molecular emission signal was
94 collected and Fourier transformed to obtain the spectrum in the
95 frequency domain. In our setup, the microwave radiation travels
96 parallel to the axis of the resonator, and consequently, all
97 transitions appear as doublets because of the Doppler effect
98 (see inlets of Figure 1). The line width in this experiment is ca.
99 5 kHz, and the accuracy of the frequency measurements is
100 better than 3 kHz.

101 ■ RESULTS AND DISCUSSION

102 **Rotational Spectra Analysis.** According to simple
103 considerations based on the expected coplanarity of the acid
104 and pyridine moieties, two possible arrangements *s-cis* or *s-trans*
105 of the $-\text{COOH}$ group relative to the N atom can be anticipated
106 for picolinic acid. In the *s-cis* configuration, in which the $-\text{OH}$
107 group and the N atom are at the same side, two conformers *s-cis*-I
108 and *s-cis*-II have to be considered. Conformer *s-cis*-I
109 presents an $\text{O}-\text{H}\cdots\text{N}$ intramolecular hydrogen bond with a
110 destabilizing $-\text{COOH}$ trans configuration, while conformer *s-*
111 *cis*-II shows a $-\text{COOH}$ cis configuration. Geometry optimiza-
112 tions for the three plausible conformers were carried out at the
113 MP2/6-311++G(d,p)²⁰ level of theory with the Gaussian suite
114 of programs,²¹ and the predicted rotational spectroscopic
115 constants are summarized in Table 1.

116 **Table 1. Plausible Conformers of Picolinic Acid Together
117 with the Calculated^a Spectroscopic Parameters and Energies**

	<i>s-cis</i> -I	<i>s-cis</i> -II	<i>s-trans</i>
A/B/C ^b	3880/ 1286/ 966	3931/ 1262/ 960	3922/ 1255/ 960
$ \mu_a / \mu_b / \mu_c $	5.8/ 0.4/ 0.0	2.4/ 0.6/ 0.3	2.3/ 3.1/ 0.0
$\chi_{aa}/\chi_{bb}/\chi_{cc}$	-0.43/ -2.49/ 2.92	-0.40/ -2.89/ 3.30	-0.21/ -3.08/ 3.29
ΔE_{MP2}	0	1175	1486
ΔG_{MP2}^d	0	1107	1497

^aAb initio calculations performed at the MP2/6-311++G(d,p) level of theory. ^bA, B, and C are the rotational constants (in MHz); χ_{aa} , χ_{bb} , and χ_{cc} are the diagonal elements of the ^{14}N nuclear quadrupole coupling tensor (in MHz); $|\mu_a|$, $|\mu_b|$, and $|\mu_c|$ are the electric dipole moment components (in D). ^cRelative electronic energies calculated at MP2/6-311++G(d,p) electronic energies (in cm^{-1}). ^dGibbs energies calculated at 298 K (in cm^{-1}).

116 The conformers of picolinic acid are near prolate asymmetric
117 tops with recognizable rotational spectrum patterns of μ_a -type
118 R-branch transitions separated by frequency intervals of
119 approximately B + C values of rotational constants. Initial
120 inspection of the broadband CP-FTMW rotational spectrum
121 shown in Figure 1a soon revealed two sets of intense R-branch
122 μ_a -type rotational transitions (with $J' \leftarrow J'' = 3 \leftarrow 2$ and $4 \leftarrow 3$)
123 belonging to a first rotamer A. Rotational transitions exhibit the

typical hyperfine structure arising from the interaction between
the electric quadrupole moment of the ^{14}N nucleus ($I = 1$) and
the electric field gradient created by all the molecular charges at
the site of this nucleus. Nevertheless, this hyperfine structure is
not well resolved by the CP-FTMW technique so only the
central frequencies were used in a rigid rotor analysis to obtain
a preliminary set of rotational constants employed in the initial
stage of the assignment procedure. μ_b - and μ_c -type transitions
were also predicted but not observed. All the assigned
rotational transitions were subsequently submitted to the high
resolution of our LA-MB-FTMW spectrometer to resolve their
hyperfine structure (see inlet of Figure 1a). Hence, a total of 30
hyperfine components belonging to nine μ_a -type R-branch
transitions were collected and fitted²² to a Hamiltonian $H = H_{\text{R}}$
 $+ H_{\text{Q}}$ where H_{R} is the rigid rotor Hamiltonian term and H_{Q} is
the nuclear quadrupole coupling interaction term.²³ The
Hamiltonian was set up in the coupled basis set $I + J = F$, so
the energy levels involved in each transition are labeled with the
quantum numbers J , K_{-1} , K_{+1} , and F . The derived spectroscopic
parameters for rotamer A are listed in Table 2. Only the

**Table 2. Spectroscopic Parameters Determined for
Rotamers of A and B of Picolinic Acid**

	rotamer A (<i>s-cis</i> -I)	rotamer B (<i>s-cis</i> -II)
A ^a (MHz)	3903.906 (16) ^d	3958.969 (17)
B (MHz)	1290.82296 (17)	1268.13439 (16)
C (MHz)	970.41622 (15)	961.33930 (15)
Δ_c (μA^2)	-0.18579(66)	-0.47279 (68)
χ_{aa} (MHz)	-0.5601 (22)	-0.5637 (38)
χ_{bb} (MHz)	-2.5718 (39)	-3.030 (16)
χ_{cc} (MHz)	3.1218 (39)	3.594 (16)
N^b	30	24
σ^c (kHz)	1.9	1.7

^aA, B, and C represent the rotational constants; $\Delta_c = (I_c - I_a - I_b) = -2\sum_i m_i c_i^2$ is the inertial defect; χ_{aa} , χ_{bb} , and χ_{cc} are elements of the ^{14}N nuclear quadrupole coupling tensor. ^bNumber of fitted hyperfine components. ^crms deviation of the fit. ^dStandard error in parentheses in units of the last digit.

diagonal elements (χ_{aa} , χ_{bb} , and χ_{cc}) of the quadrupole coupling
tensor χ were determined in the fit of the observed transitions
within the estimated accuracy of the frequency measurements.
The anisotropic quadrupole coupling tensor χ is related to the
electric field gradient tensor q at the quadrupolar nucleus
through the nuclear quadrupole moment eQ by $\chi = eQq$.

The high sensitivity reached in our experiment allowed us to
extend the spectral measurements to five monosubstituted ^{13}C ,
 ^{15}N , and one ^{18}O species observed in their natural abundances
(approximately 1%, 0.4%, and 0.2%) for the A rotamer (see
Figure 1b). The analysis of the ^{13}C spectra was performed with
the same Hamiltonian used for the parent species. For the ^{15}N
species no quadrupole coupling interaction takes place so its
spectrum does not show hyperfine structure. The ^{18}O species
was only observed using the CP-FTMW spectrometer and thus
its quadrupole coupling hyperfine structure was not resolved.
The derived spectroscopic parameters for the isotopic species
are collected in Table 3.

Once the analysis of the parent and isotopic species of
rotamer A was completed and the lines discarded from the
rotational spectra, very weak μ_a -type R-branch transitions,
belonging to a second rotamer B, were identified. The
intensities of the transitions are similar to those observed for

Table 3. Experimental Spectroscopic Parameters for the Observed Isotopic Species of Rotamer A of Picolinic Acid

	C ₁	C ₄	C ₅	C ₆	C ₇	¹⁵ N	¹⁸ O
A ^a (MHz)	3860.328 (16)	3856.905 (10)	3863.912 (12)	3903.771 (16)	3903.719 (19)	3865.356 (17)	3832.35 (41)
B (MHz)	1281.01642 (17)	1289.77504 (10)	1278.27790 (12)	1269.79114 (17)	1281.84845 (19)	1290.33767 (18)	1257.0929 (64)
C (MHz)	962.17613 (17)	966.89405 (10)	960.85157 (12)	958.47311 (16)	965.32392 (18)	967.74067 (18)	946.9194 (43)
Δ _c (μÅ ²)	-0.1843 (7)	-0.1843 (4)	-0.1840 (5)	-0.1858 (7)	-0.1858 (8)	-0.184 (16)	-0.185 (19)
χ _{aa} (MHz)	-0.5366 (27)	-0.5744 (25)	-0.6259 (29)	-0.568 (15)	-0.5557 (29)		
χ _{bb} (MHz)	-2.6033 (65)	-2.540 (10)	-2.516 (12)	-2.583 (22)	-2.5784 (60)		
χ _{cc} (MHz)	3.1399 (65)	3.115 (10)	3.1418 (12)	3.151 (22)	3.1340 (60)		
N ^b	26	24	23	19	27	9	5
σ ^c (kHz)	1.9	1.1	1.3	1.7	2.1	1.2	24.9

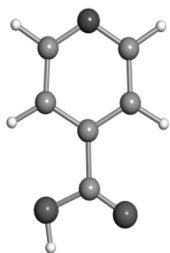
^aA, B, and C represent the rotational constants; Δ_c is the inertial defect; χ_{aa}, χ_{bb}, and χ_{cc} are elements of the ¹⁴N nuclear quadrupole coupling tensor. ^bNumber of fitted hyperfine components. ^crms deviation of the fit. ^dStandard error in parentheses in units of the last digit.

¹³C species of rotamer A, as can be seen in Figure 1b for the 3₁₂-2₁₁ transition. No μ_b- and μ_c-type transitions were observed. A total of 24 hyperfine components corresponding to the detected nine μ_a-type R-branch transitions were measured using LA-MB-FTMW spectroscopy and analyzed with the same Hamiltonian mentioned above. The final set of rotational and nuclear quadrupole coupling constants are listed in the second column of Table 2.

The spectrum of isonicotinic acid has been investigated following a similar procedure to that described for picolinic acid. Differently from picolinic acid (*ortho*-COOH substituted), in isonicotinic acid (*para*-COOH substituted), only the conformer in Table 4 can be expected. Hence, the broadband

Table 4. Calculated^a and Experimental Spectroscopic Parameters for the Observed Rotamer of Isonicotinic Acid

	Isonicotinic acid	
	Theor.	Exp.
A ^b /MHz	4006	4027.83775 (63) ^e
B/MHz	1213	1219.95126 (12)
C/MHz	933	937.018821 (90)
Δ _c /μÅ ²	-1.3	-0.38541 (11)
μ _a /D	1.4	Obs. ^f
μ _b /D	1.2	Obs.
μ _c /D	0.1	
χ _{aa} /MHz	-4.94	-5.0395 (46)
χ _{bb} /MHz	1.50	1.3574 (44)
χ _{cc} /MHz	3.44	3.6822 (44)
N ^c		38
σ ^d /kHz		1.6



^aAb initio calculations performed at the MP2/6-311++G(d,p) level of theory. ^bA, B, and C are the rotational constants; Δ_c = (I_c - I_a - I_b) = -2Σ_im_ic_i² is the inertial defect; |μ_a|, |μ_b|, and |μ_c| are the electric dipole moment components; χ_{aa}, χ_{bb}, and χ_{cc} are the diagonal elements of the ¹⁴N nuclear quadrupole coupling tensor. ^cNumber of fitted hyperfine components. ^drms deviation of the fit. ^eStandard error in parentheses in units of the last digit. ^fObservation of a- and b-type spectra.

CP-FTMW rotational spectrum of Figure 2 only shows sets of intense R-branch μ_a- and μ_b-type rotational transitions attributable to one rotamer of isonicotinic acid. A total of 25 ¹⁴N hyperfine components from nine μ_a-type R-branch transitions and 13 corresponding to five μ_b-type R-branch transitions were resolved and measured using LA-MB-FTMW spectroscopy (see inlet of Figure 2). All hyperfine components were fitted using the same Hamiltonian as described for picolinic acid. The determined spectroscopic parameters are also shown in Table 4. All frequency measurements for picolinic and isonicotinic acids are provided as Supporting Information (Table S1–S10).

Conformational Identification and Structure. Conformational identification is commonly achieved by comparing the experimentally determined molecular properties with those predicted ab initio.²⁴ In particular, the rotational constants (A, B, C), the ¹⁴N nuclear quadrupole coupling constants (χ_{aa}, χ_{bb}, χ_{cc}), and the values of the electric dipole moment components along the principal inertial axis (μ_a, μ_b, μ_c) should all be consistent with ab initio values, even if only one of these tools is acting as the discriminating element.

The values of the rotational constants depend on the mass distribution around the principal inertial axes, so they are commonly used as conclusive tool in the identification of the observed species. In picolinic acid, the experimental values for A and B rotamers in Table 2 are similar to those predicted for *s-cis*-I, *s-cis*-II, and *s-trans* conformers in Table 1, thus making their assignment difficult. The same works for the ¹⁴N nuclear quadrupole coupling constants. This is reflected in nearly identical quadrupole hyperfine patterns for both A and B rotamers, as can be seen in the insets of Figure 1 for the same 3₁₂-2₁₁ rotational transition. On this basis, the two observed rotamers can be ascribed to the lowest energy conformers, but an unambiguous identification to specific conformers cannot be achieved using rotational and quadrupole coupling constants as conformational tools.

The nonobservation of μ_b-type spectra for rotamers A and B and the predicted low values of the μ_b electric dipole moment component for conformers *s-cis*-I and *s-cis*-II points to the presence of these conformers in the supersonic expansion. On the same basis, conformer *s-trans* should be discarded due to the predicted high value of the μ_b dipole moment component. Conformer *s-cis*-I is predicted to be, by far, the most stable conformer of picolinic acid in accordance with the intense observed rotational spectrum for rotamer A. Additionally, the predicted changes in the rotational constants going from *s-cis*-I to *s-cis*-II are ΔA ≈ 50.9 (55.1) MHz, ΔB ≈ -23.62 (-22.7) MHz, and ΔC ≈ -6.0 (-9.1) MHz, which match nicely with those experimentally observed (in parentheses) in going from rotamer A to rotamer B. This allows the identification of rotamers A and B as conformers *s-cis*-I and *s-cis*-II, respectively. For isonicotinic acid, the predicted values of the rotational and quadrupole coupling constants for the most stable species (see Table 4) are in excellent agreement with those experimentally observed.

The inertial defect values Δ_c in Table 2 obtained for the observed conformers give a measure of the mass extension out of the *ab* plane. While for planar rigid molecules Δ_c should be strictly zero, the ground state vibrational motions give rise to inertial defect values, which are negative and close to zero.^{25–27}

Hence, the planarity of all conformers is confirmed by the experimental values of the inertial defect Δ_c (see Table 2). The differences in the experimental inertial defect values for picolinic acid conformers *s-cis-I* and *s-cis-II* and isonicotinic acid can be rationalized if we compare them with those observed for related planar pyridine,²⁸ benzoic acid,²⁹ or nicotinic acid.¹⁴ Hence, while in pyridine Δ_c is very small and positive ($\Delta_c = 0.039 \mu\text{Å}^2$), the negative values observed for the rest of them collected in Table 6 indicates that out-of-plane vibrations related to the presence of $-\text{COOH}$ group have dominant contributions.

A close look to the values in Table 6 shows that the inertial defect for conformer *s-cis-I* ($\Delta_c = -0.186 \mu\text{Å}^2$) is roughly half the value of benzoic ($\Delta_c = -0.366 \mu\text{Å}^2$), nicotinic ($\Delta_c = -0.352 \mu\text{Å}^2$ and $\Delta_c = -0.374 \mu\text{Å}^2$ for conformers *s-cis* and *s-trans*, respectively) and isonicotinic acids ($\Delta_c = -0.38541 \mu\text{Å}^2$), which is, in turn, smaller than the inertial defect for conformer *s-cis-II* ($\Delta_c = -0.473 \mu\text{Å}^2$). In other words we can affirm that the out of plane vibrational contributions of $-\text{COOH}$ in *s-cis-I* are smaller than in the rest of species. This is in accordance with the observation of an intramolecular $\text{O}-\text{H}\cdots\text{N}$ hydrogen bond in the *s-cis-I* conformer, which limits in some extent the amplitude of the out-of-plane $-\text{COOH}$ vibration in this conformer. The fact that the Δ_c value observed for conformer *s-cis-II* is slightly higher than those of benzoic acid, nicotinic acid, or isonicotinic acid may be explained in terms of the $\text{N}\cdots\text{O}$ repulsions, which would contribute to increase the amplitude of the out-of-plane $-\text{COOH}$ vibrations in this conformer. These $\text{N}\cdots\text{O}$ repulsions are not present in the meta and para positions of the $-\text{COOH}$ groups in nicotinic and isonicotinic acids.

Finally, it should be noted that the value of the inertial defect is practically invariant in all the isotopic species (Table 3), which constitutes an additional test for the planarity of the *s-cis-I* conformer. This isotopic information was used to determine the coordinates of the substituted atoms in the principal axis system using Kraitchmann's substitution method^{30–32} and to determine the bond distances and angles of the heavy atom skeleton listed in Table 5.

Quadrupole Coupling Constants: Intramolecular Hydrogen Bonding and Mesomeric Effect. An inspection of the experimental values of the nuclear quadrupole coupling constants could reveal interesting information on the different

nature of the observed conformers. The ^{14}N nucleus present in all the conformers possess a nonzero quadrupole moment ($I = 2$) owing to a nonspherical distribution of the nuclear charge, which interacts with the electric field gradient created by the rest of the molecule at the site of the nucleus. The associated experimentally determinable molecular properties are the diagonal elements (χ_{aa} , χ_{bb} , χ_{cc}) of the nuclear quadrupole coupling tensor that are directly related to the electronic environment around the nitrogen nucleus referred to the principal inertial axes. For planar molecules, like those of isomeric picolinic, nicotinic,¹⁴ and isonicotinic acids, the χ_{cc} element of the quadrupole coupling tensor is coincident with one of the elements of the principal quadrupole coupling tensor and provides information on the electric field gradient along the direction of an axis perpendicular to the aromatic ring. For pyrrolic nitrogens ($-\text{N}<$) χ_{cc} is negative.^{33–35} In contrast, pyridinic nitrogens ($-\text{N}=\text{}$) have positive values of χ_{cc} .^{34–36} Conformer *s-cis-I* and *s-cis-II* of picolinic acid have positive values for χ_{cc} indicating their pyridinic nature. However, while conformer *s-cis-II* presents a value for χ_{cc} of 3.594 MHz very close to that of pyridine (see Table 6), a markedly lower value of 3.122 MHz is found for the *s-cis-I* conformer. This difference cannot be attributed to possible changes in the orientation of the principal inertial axes; both conformers differ only in the orientation of the hydroxyl group. It must be ascribed to the formation of an intramolecular hydrogen bond $\text{O}-\text{H}\cdots\text{N}$ in the *s-cis-I* conformer, which increase slightly the pyrrolic character of the nitrogen nucleus by diminishing the χ_{cc} value.

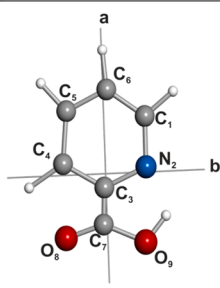
A more detailed analysis of the nuclear quadrupole coupling constants shows small discrepancies in the χ_{cc} values in passing from *ortho*- and *para*- COOH substituted species to the *meta*- COOH ones. Hence, in the case of *s-cis-II* picolinic (*ortho*- COOH substituted) and isonicotinic (*para*- COOH substituted) acids, one observes a small increase of the χ_{cc} with respect to the values of nicotinic *s-cis* or *s-trans*¹⁴ (*meta*- COOH substituted), which adopt practically the same value as for pyridine (see Table 6). Here an effect based on the exchange interaction of the lone electron pairs of the $-\text{COOH}$ substituent with the π electrons of the pyridine ring³⁶ can be considered. This type of electron shift is termed mesomeric effect^{37,38} and is signified by $-M$ or $+M$, depending on whether the electron shift takes place from the aromatic ring to the substituent ($-M$) or in the reverse direction ($+M$). In the case of the isomeric series of picolinic, nicotinic, and isonicotinic acids, the electron distribution shift is in favor of the carboxylic group ($-M$), extracting electrons from the π -ring system in *ortho* and *para* positions (see Figure 3), which is reported by a small but noticeable increase in the χ_{cc} values of about 0.2 MHz. For the *s-cis-I* conformer, the decrease in the value of χ_{cc} with respect to *s-cis-II* conformer might be due to a negative polarization at the N atom arising from the formation of a $-\text{COOH}\cdots\text{N}$ hydrogen bond.

CONCLUSIONS

In this work, two of the three plausible conformers of picolinic acid and the only plausible conformer for isonicotinic acid have been observed. For the most stable conformer of picolinic acid *s-cis-I* the heavy atom skeleton structure has been determined from the observation of ^{13}C , ^{18}O , and ^{15}N isotopologues in natural abundance using the CP-FTMW spectrometer. The formation of an intramolecular $\text{O}-\text{H}\cdots\text{N}$ hydrogen bond in the most stable conformer of picolinic acid has been also revealed by its signatures in the quadrupole coupling constants and the

Table 5. Substitution Coordinates and r_s Structure for Conformer *s-cis-I* of Picolinic Acid

atom	[a]	[b]	[c] ^a
C ₁	1.73073 (69) ^b	1.21898 (98)	0
N ₂	0.3847 (31)	1.1396 (11)	0
C ₃	-	-	-
C ₄	0.5643 (21)	1.26006 (95)	0
C ₅	1.96007 (61)	1.1692 (10)	0
C ₆	2.55258 (47)	0.068 (18)	0
C ₇	1.65955 (72)	0.079 (15)	0
O ₈	2.29744 (52)	1.1289 (11)	0
$r(\text{C}_1-\text{N}_2)$	1.35 (39) ^d	$\angle\text{C}_4-\text{C}_5-\text{C}_6$	119.32 (47)
$r(\text{C}_6-\text{C}_1)$	1.41 (16)	$\angle\text{C}_5-\text{C}_6-\text{C}_1$	118.88 (22)
$r(\text{C}_5-\text{C}_6)$	1.37 (17)	$\angle\text{C}_6-\text{C}_1-\text{N}_2$	122.15 (57)
$r(\text{C}_4-\text{C}_5)$	1.40 (29)		
$r(\text{C}_7-\text{O}_8)$	1.23 (14)		



^aPlanar structure has been assumed. ^bPrincipal inertial axis coordinates in Å; derived errors in parentheses in units of the last digit; These were calculated according to Constains formula: $\sigma(x) = K/|x|$; $\sigma(x)$ is the error in the x coordinate and $K = 0.0012 \text{ Å}^2$. ^cThe rotational transitions of the ^{13}C species of the C₃ carbon atom are so close to those of the parent species that become undetectable. ^dDistances in Å and angles in degrees.

Table 6. Experimental Inertial Defects (in $\mu\text{Å}^2$) and ^{14}N Quadrupole Coupling Constants (in MHz) of Picolinic and Isonicotinic Acids Compared to Those of Nicotinic Acid, Benzoic Acid, and Pyridine

	Picolinic acids-cis-I	Picolinic acid s-cis-II	Isonicotinic acid	Nicotinic acid s-cis	Nicotinic acid s-trans	Benzoic acid	Pyridine
Δ_c	-0.186 ^a	-0.473 ^a	-0.385 ^a	-0.352 ^b	-0.374 ^b	-0.366 ^c	0.039 ^d
χ_{cc}	3.122 ^a	3.594 ^a	3.682 ^a	3.422 ^b	3.453 ^b	-	3.474 ^e

^aPresent work. ^bFrom ref 14. ^cFrom ref 29. ^dFrom ref 28. ^eFrom ref 36.

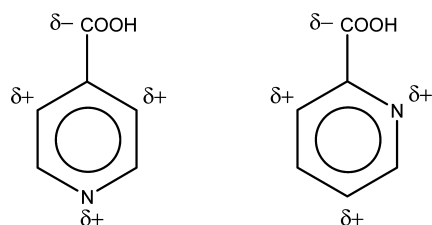


Figure 3. Resonance withdrawing effect in picolinic (left) and isonicotinic (right) acids.

ACKNOWLEDGMENTS

This work has been supported by the Ministerio de Ciencia e Innovación (Grants CTQ2010-19008 and Consolider-Ingenio 2010 CSD2009-00038) and Junta de Castilla y León (Grant VA175U13). C.C. thanks the Junta de Castilla y León for a postdoctoral contract (Grant CIP13/01).

REFERENCES

- Iwata, K.; Ogata, S.; Okumura, K.; Taguchi, H. Induction of Differentiation in Human Promyelocytic Leukemia HL-60 Cell Line by Niacin-related Compounds. *Biosci. Biotechnol. Biochem.* **2003**, *67* (5), 1132–1135.
- Grant, R. S.; Coggan, S. E.; Smythe, G. A. The Physiological Action of Picolinic Acid in the Human Brain. *Int. J. Tryptophan Res.* **2009**, *2*, 71–79.
- Dazzi, C.; Candiano, G.; Massazza, S.; Ponzetto, A.; Varesio, L. New High-Performance Liquid Chromatographic Method for the Detection of Picolinic Acid in Biological Fluids. *J. Chromatogr. B: Biomed. Sci. Appl.* **2001**, *751*, 61–68.
- Smythe, G. A.; Braga, O.; Brew, B. J.; Grant, R. S.; Guillemin, G. J.; Kerr, S. J.; Walker, D. W. Concurrent Quantification of Quinolinic, Picolinic, and Nicotinic Acids Using Electron-Capture Negative-Ion Gas Chromatography Mass Spectrometry. *Anal. Biochem.* **2002**, *301*, 21–26.
- Rebello, T.; Lonnerdal, B.; Hurley, L. S. Picolinic Acid in Milk, Pancreatic Juice, and Intestine: Inadequate for Role in Zinc Absorption. *Am. J. Clin. Nutr.* **1982**, *35*, 1–5.
- Paris, M.; Thomas, G.; Merlin, J. C. Structure de l'Acide Picolique. *Bull. Soc. Chim. France* **1961**, 707–719.
- Hamann, S. D. The Influence of Pressure on the Infrared Spectra of Hydrogen-Bonded Solids. The Formation of Fermi Resonance 'Windows'. *Aust. J. Chem.* **1977**, *30*, 71–9.
- Imai, Y.; Kurokawa, Y.; Hara, M.; Fukushima, M. Observation of SERS of Picolinic Acid and Nicotinic Acid Using Cellulose Acetate Films Doped with Ag Fine Particles. *Spectrochim. Acta, Part A* **1997**, *53*, 1697–1700.
- Spinner, E. A Strongly Hydrogen-Bonded Molecular Solid, Isonicotinic Acid: Raman Spectra of the $-\text{C}''\text{O,H}$ and $-\text{C}''\text{O,D}$ Species and Infrared and Raman Spectra of the $-\text{C}''\text{O,H}$ Acid. *J. Phys. Chem.* **1988**, *92*, 3379–3386.
- Park, S. M.; Kim, K.; Kim, M. S. Raman Spectroscopy of Isonicotinic Acid Adsorbed onto Silver Sol Surface. *J. Mol. Struct.* **1994**, *328*, 169–178.
- Koczon, P.; Dobrowolski, J. Cz.; Lewandowski, W.; Mazurek, A. P. Experimental and Theoretical IR and Raman Spectra of Picolinic, Nicotinic and Isonicotinic Acids. *J. Mol. Struct.* **2003**, *65*, 89–95.
- Takusagawa, F.; Shimada, A. The Crystal Structure of Picolinic Acid. *Chem. Lett.* **1973**, 1089–1090.
- Takusagawa, F.; Shimada, A. Isonicotinic Acid. *Acta Crystallogr.* **1976**, *B32*, 1925.
- Mata, S.; Peña, I.; Cabezas, C.; López, J. C.; Alonso, J. L. A Broadband Fourier-Transform Microwave Spectrometer with Laser Ablation Source: The Rotational Spectrum of Nicotinic Acid. *J. Mol. Spectrosc.* **2012**, *280*, 91–96.

vibrational contributions to the inertial defect values. The formation of this hydrogen bond forces the $-\text{COOH}$ group to adopt a trans configuration, considerably less stable than its usual *cis* configuration. The stabilization energy provided by this hydrogen bond interaction thus compensates the destabilization due to the adoption of a $-\text{COOH}$ trans configuration.

The role of the quadrupole coupling constants has been also found to be essential to detect the subtle effects of exchange interactions in aromatic systems. Hence, mesomeric effect from $-\text{COOH}$ group in ortho and para positions has been unveiled in picolinic and isonicotinic acids by comparing the χ_{cc} values of the quadrupole coupling constants to those found for nicotinic acid and pyridine molecules.

It has been shown that the combination of laser ablation with the chirped-pulse Fourier transform microwave spectroscopy (CP-FTMW) provides an efficient tool in the analysis of the rotational spectra of biomolecules with high melting points. This technique is complementary to LA-MB-FTMW spectroscopy with superior resolution to resolve the hyperfine structure. Both techniques constitute sensitive tools for the structure determination of biomolecules.

ASSOCIATED CONTENT

Supporting Information

Complete ref 21, list of measured transitions for the observed conformers of picolinic and isonicotinic acids, and ab initio coordinates and structural parameters for conformer *s-cis-I* of picolinic acid. This material is available free of charge via the Internet at <http://pubs.acs.org>.

AUTHOR INFORMATION

Corresponding Author

*E-mail: jjalonso@qf.uva.es. Tel: +34 983186345.

Notes

The authors declare no competing financial interest.

- 431 (15) Alonso, J. L.; Pérez, C.; Sanz, M. E.; López, J. C.; Blanco, S.
432 Seven Conformers Of L-Threonine in the Gas Phase: A LA-MB-
433 FTMW Study. *Phys. Chem. Chem. Phys.* **2009**, *11*, 617–627.
- 434 (16) Cabezas, C.; Varela, M.; Peña, I.; Mata, S.; López, J. C.; Alonso,
435 J. L. The Conformational Locking of Asparagine. *Chem. Commun.*
436 **2012**, *48*, 5934–5936 and references therein..
- 437 (17) Puzzarini, C.; Biczysko, M.; Barone, V.; Largo, L.; Peña, I.;
438 Cabezas, C.; Alonso, J. L. Accurate Characterization of the Peptide
439 Linkage in the Gas Phase: A Joint Quantum-Chemical and Rotational
440 Spectroscopy Study of the Glycine Dipeptide Analogue. *J. Phys. Chem.*
441 *Lett.* **2014**, *5*, 534–540 and references therein..
- 442 (18) Alonso, J. L.; Peña, I.; López, J. C.; Vaquero, V. Rotational
443 Spectral Signatures of Four Tautomers of Guanine. *Angew. Chem., Int.*
444 *Ed.* **2009**, *48*, 6141–6143 and references therein..
- 445 (19) Alonso, J. L.; Lozoya, M.; Peña, I.; López, J. C.; Cabezas, C.;
446 Mata, S.; Blanco, S. The Conformational Behaviour of Free D-Glucose-
447 at Last. *Chem. Sci.* **2014**, *5*, 515–522.
- 448 (20) Møller, C.; Plesset, M. S. Note on an Approximation Treatment
449 for Many-Electron Systems. *Phys. Rev.* **1934**, *46*, 618–622.
- 450 (21) Frisch, M. J.; Trucks, G. W.; Schlegel, H. B.; Scuseria, G. E.;
451 Robb, M. A.; Cheeseman, J. R.; Scalmani, G.; Barone, V.; Mennucci,
452 B.; Petersson, G. A.; et al. *Gaussian 09*, revision B.01; Gaussian, Inc.:
453 Wallingford, CT, 2010.
- 454 (22) Pickett, H. M. The Fitting and Prediction of Vibration-Rotation
455 Spectra with Spin Interactions. *J. Mol. Spectrosc.* **1991**, *148*, 371.
- 456 (23) Gordy, W.; Cook, R. L. In *Microwave Molecular Spectra*, 3rd ed.;
457 Weissberg, A., Ed.; Techniques of Chemistry; John Wiley & Sons Inc.:
458 New York, 1984; Vol. XVIII.
- 459 (24) Peña, I.; Sanz, M. E.; López, J. C.; Alonso, J. L. Preferred
460 Conformers of Proteinogenic Glutamic Acid. *J. Am. Chem. Soc.* **2012**,
461 *134*, 2305–2312 and references therein..
- 462 (25) Oka, T. On Negative Inertial Defect. *J. Mol. Struct.* **1995**, *352*/
463 *353*, 225–233.
- 464 (26) Jagod, M.-F.; Oka, T. Inertial Defects of Planar Symmetric Top
465 Molecules. *J. Mol. Spectrosc.* **1990**, *139*, 313–327.
- 466 (27) Oka, T.; Morino, Y. Inertial Defect. Part III. Inertia Defect and
467 Planarity of Four-Atomic Molecules. *J. Mol. Spectrosc.* **1963**, *11*, 349–
468 367.
- 469 (28) Ye, E.; Bettens, R. P. A.; De Lucia, F. C.; Petkie, D. T.; Albert, S.
470 Millimeter and Submillimeter Wave Rotational Spectrum of Pyridine
471 in the Ground and Excited Vibrational States. *J. Mol. Spectrosc.* **2005**,
472 *232*, 61–65.
- 473 (29) Onda, M.; Asai, M.; Takise, K.; Kuwae, K.; Hayami, K.; Kuroe,
474 A.; Mori, M.; Miyazaki, H.; Suzuki, N.; Yamaguchi, I. Microwave
475 Spectrum of Benzoic Acid. *J. Mol. Struct.* **1999**, *482–483*, 301–303.
- 476 (30) Kraitchmann, J. Determination of Molecular Structure from
477 Microwave Spectroscopic Data. *Am. J. Phys.* **1953**, *21*, 17–24.
- 478 (31) Costain, C. C. Determination of Molecular Structures from
479 Ground State Rotational Constants. *J. Chem. Phys.* **1958**, *29*, 864.
- 480 (32) Van Eijck, B. P. Influence of Molecular Vibrations on
481 Substitution Coordinates. *J. Mol. Spectrosc.* **1982**, *91*, 348–362.
- 482 (33) Bohn, R. K.; Hillig, K. W., II; Kuczkowski, R. L. Pyrrole-Argon:
483 Microwave Spectrum, Structure, Dipole Moment, and ¹⁴N Quadrupole
484 Coupling Constants. *J. Phys. Chem.* **1989**, *93*, 3456–3459.
- 485 (34) Tanjaroon, C.; Subramanian, R.; Karunatilaka, C.; Kukulich, S.
486 G. Microwave Measurements of ¹⁴N and D Quadrupole Coupling for
487 (Z)-2-Hydroxypyridine and 2-Pyridone Tautomers. *J. Phys. Chem. A*
488 **2004**, *108*, 9531–9539.
- 489 (35) Stolze, M.; Sutter, D. H. The Rotational Zeeman Effect of
490 Pyrazole and Imidazole. *Z. Naturforsch. A* **1987**, *42a*, 49–56.
- 491 (36) Heineking, N.; Dreizler, H.; Schwarz, R. Nitrogen and
492 Deuterium Hyperfine Structure in the Rotational Spectra of Pyridine
493 and [4-D] Pyridine. *Z. Naturforsch. A* **1986**, *41a*, 1210–1213.
- 494 (37) Schmidt, A. Biologically Active Mesomeric Betaines and
495 Alkaloids Derived from 3-Hydroxypyridine, Pyridin-N-oxide, Nicotinic
496 Acid and Picolinic Acid. Three Types of Conjugation and their
497 Consequences. *Curr. Org. Chem.* **2004**, *8*, 653.
- 498 (38) McMurry, J. E. *Organic Chemistry*, 8th ed; Cengage Learning:
499 Independence, KY, 2012.